

Saturation of the Neutron Yield from Megajoule Plasma Focus Facilities

V. Ya. Nukulin and S. N. Polukhin

Lebedev Institute of Physics, Russian Academy of Sciences, Leninskii pr. 53, Moscow, 119991 Russia

Received May 16, 2006

Abstract—A relation is investigated between the saturation of the neutron yield from megajoule plasma focus facilities and that of the total discharge current. An analytic formula for the neutron yield as a function of the facility energy is derived by simple calculations of the discharge circuit and is verified by computer simulations of the dynamics of the current sheath. The dependence obtained differs from the generally accepted one but agrees well with experimental data.

PACS numbers: 52.58.Lq, 52.59.Hq, 52.70.-m

DOI: 10.1134/S1063780X07040022

1. INTRODUCTION

When describing the neutron yield from plasma focus (PF) facilities, the following two scalings are usually used, which relate the neutron yield Y_n to (i) the energy E [J] stored in the capacitor bank and (ii) the discharge current I_p [A] at the instant of pinching [1–3]:

$$Y_n \approx 10E^2, \quad (1)$$

$$Y_n \approx 10^{-13} I_p^4. \quad (2)$$

These scalings were obtained experimentally in the 1970s–1990s in facilities with stored energies of 1–100 kJ and raised hope that a PF would be used as a prototype thermonuclear reactor, provided that the stored energy could be increased by two to three orders of magnitude. It was then found, however, that the neutron yield was saturated when passing to the megajoule energy range: instead of the expected 10^{13} neutrons per shot, the neutron yield was at least ten times lower [4], although current scaling (2) usually remained valid. The commonly accepted explanation of this effect (which is, however, difficult to verify experimentally) is based on the hypothesis that the pinch current is shunted by the peripheral plasma. Putting aside this problem, we will consider here only the electrotechnical factors that lead to the saturation of the discharge current with increasing the stored energy, thereby decreasing the neutron yield as compared to the expected value.

Since there are many reasons why neutron measurements in the megajoule energy range have been usually performed in Mather-type PF facilities, we will deal here (unless otherwise stated) just with this type of PF.

2. NEUTRON YIELD IN THE KILOJOULE ENERGY RANGE

From the electrotechnical standpoint, a PF discharge represents damping current oscillations in an LC circuit (Fig. 1) with the inductance $L = L_c + L_t$, where L_c is the inductance of the capacitor bank and feeding cables and L_t is the growing inductance of the discharge chamber, current sheath (CS), and pinch. In kilojoule PFs, the discharge inductance is determined by the inductance of the capacitor bank and feeding cables; i.e., the inductance of the discharge chamber and plasma column can be ignored, except for the short time interval near the so-called “singularity” in the current time derivative. For example, in the PF-4M facility [5] (Lebedev Physical Institute) with a stored energy of 15 kJ ($C = 48 \mu\text{F}$, $U = 10\text{--}20$ kV) and a total discharge inductance (evaluated from the oscillation period, see Fig. 2) of 60 nH, the “geometrical” inductance of the electrode (anode–cathode) system is 15 nH. The pinch inductance determined from the pinch size in photographs taken with an image-converter tube is 5–7 nH. Hence, the current amplitude for such an LC circuit can be found (ignoring the resistance of the pinch and feeding cables) by the well-known formula

$$I_{\max} = U_0 \sqrt{\frac{C}{L_c}} = \sqrt{\frac{2E}{L_c}}. \quad (3)$$

Taking into account the resistance gives rise to a minor exponential factor, which reduces the maximum current in the first half-period by 10–20%.

Obviously, of the two above neutron scalings, only scaling (2), which relates the neutron yield to the discharge current, has physical meaning. This scaling reflects the key role the magnetic fields play in all the phenomena accompanying a PF discharge. In fact, energy scaling (1) is a consequence of current scaling (2).

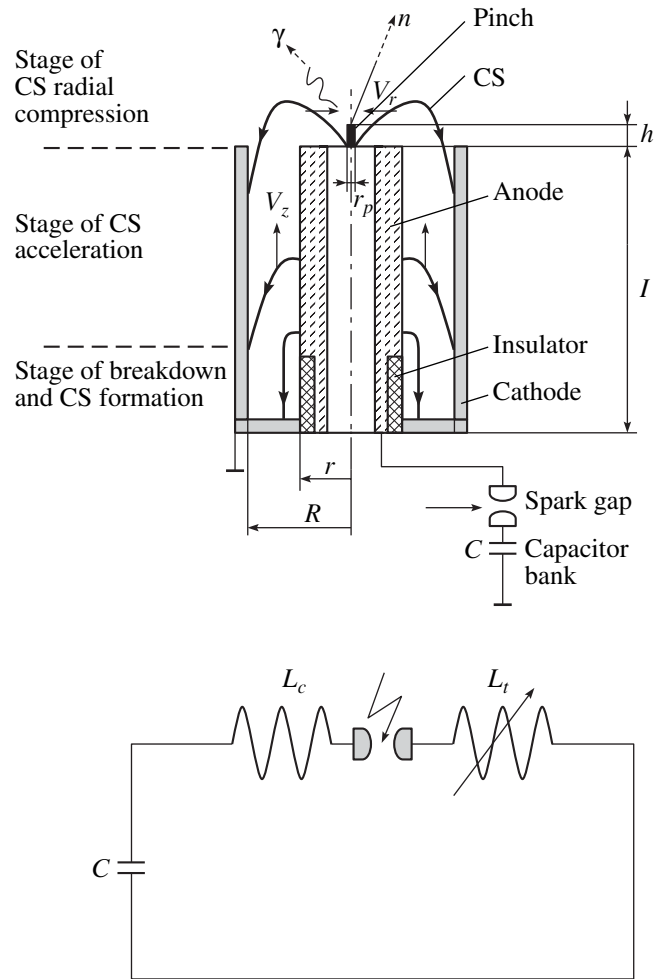


Fig. 1. Schematic of a PF facility and its equivalent electric circuit.

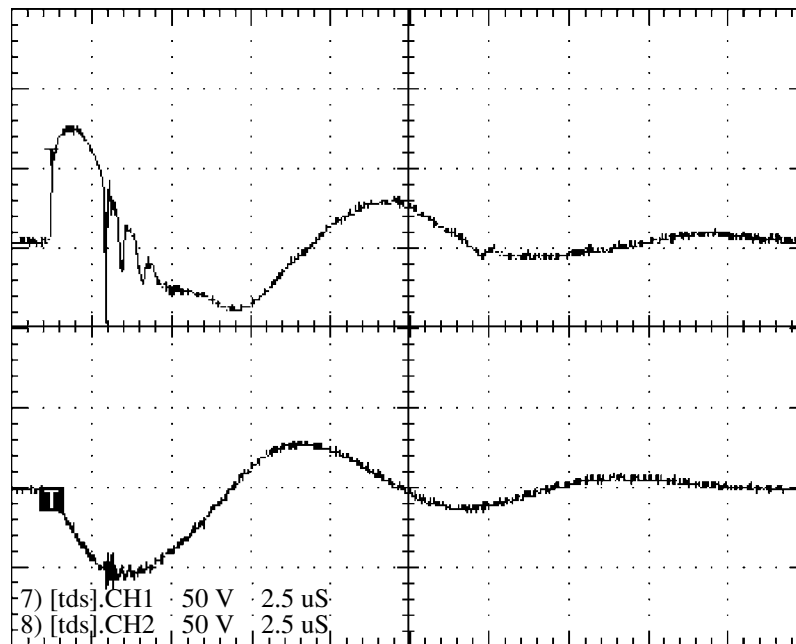


Fig. 2. Oscillograms of the FP current (lower trace) and its time derivative (upper trace). The time scale is 2.5 μ s/division.

Table

	PF-1000, 2004	Frascati 1-MJ PF, 1979–1981		PF-3
Stored energy E , MJ	0.5–0.7	0.2–0.5		0.5–1
Capacitance of the capacitor bank C , μF	1332	1300		9200
Charging voltage U , kV	30–33	20–28		10–15
Short-circuit current, MA	12	–		18
Maximum current I_{max} , MA	1.8–2	2.2–2.7		4
Pinch current I_p , MA	1.2	1.2–1.7		3
Pinching time t , μs	8.5	5.5–8.5		15–16
Invariable inductance L_c , nH	15	16–20		15
Chamber inductance L_f , nH	60	–	45	8
Cathode radius R , cm	20	45	24	58
Anode radius r , cm	11.3	37	16	50
Anode length l , cm	56	35	56	26
Insulator radius, cm	12.8	–	18	50
Insulator length, cm	11.3	5–10	15–20	26
Neutron yield Y_n	2×10^{11}	6×10^{11}	10^{12}	–
Chamber type	M	F–M	M	F

The relationship between these scalings can easily be traced in the kilojoule energy range. Let us substitute (3) into (2) and roughly assume that $I_p \approx (2/3)I_{\text{max}}$ and $L_c \approx 10^{-7}$ H; then, we obtain $Y_n \approx 10^{-13} I_p^4 = 8E^2$ (cf. scaling (1)). Thus, in the kilojoule energy range, scalings (1) and (2) agree well with one another, the former being merely a consequence of the latter.

3. NEUTRON YIELD IN THE MEGAJOULE ENERGY RANGE

In the megajoule energy range, the relationship between the current and the stored energy is no longer determined by relation (3); hence, energy scaling (1) fails to hold. At present, this seems rather obvious. An increase in the stored energy at a constant charging voltage of the capacitor bank is achieved by increasing the number of capacitors connected in parallel and, hence, is accompanied by a decrease in the inductance of the capacitor bank. On the other hand, an increase in the capacitance of the energy storage bank increases the discharge duration and inevitably causes one to lengthen the discharge electrodes in order to provide synchronism between the arrival of the CS at the facility axis and the instant of the maximum current. As a result, the relationship between L_c and L_f becomes opposite to that in the kilojoule range, namely, $L_c \ll L_f$ ($L_c \sim 10^{-8}$ H and $L_f \sim 10^{-7}$ H). In this case, the current amplitude is determined by the chamber inductance rather than by the inductance of the capacitor bank. A further increase in the capacitance of the energy storage bank does not lead to an increase in the discharge current because of the growth of the chamber inductance.

Therefore, the current and, accordingly, the neutron yield saturate.

Let us illustrate this for two large PF facilities: the PF-1000 facility at the Institute of Plasma Physics and Laser Microfusion (Warsaw) [6] and the 1-MJ PF at the CNEN Frascati Center (Roma) [4], the parameters of which are given in the table. The third column in the table presents the parameters of the PF-3 Filippov-type facility created at the Kurchatov institute [7].

Let us estimate the maximum discharge current in a Mather-type PF. In order for the current rise time t to coincide with the time at which the CS arrives at the discharge axis, the following condition must be satisfied:

$$t = \frac{\pi}{2} \sqrt{L_f C} = l/v_z, \quad (4)$$

where l is the anode length and v_z is the average axial velocity of the CS in the rundown stage. For simplicity, we ignore the stage of CS radial compression in a Mather-type PF and assume the discharge inductance to be equal to the chamber inductance L_f .

$$L_f = 2l \ln(R/r) \text{ [nH]}, \quad (5)$$

where R and r are the cathode and anode radii, respectively. In this approximation, the maximum discharge current is equal to

$$I_{\text{max}} \approx U_0 \sqrt{\frac{C}{L_f}}. \quad (6)$$

Note that, if we replace L_f with L_c , then we obtain the short-circuit current of the capacitor bank, which is

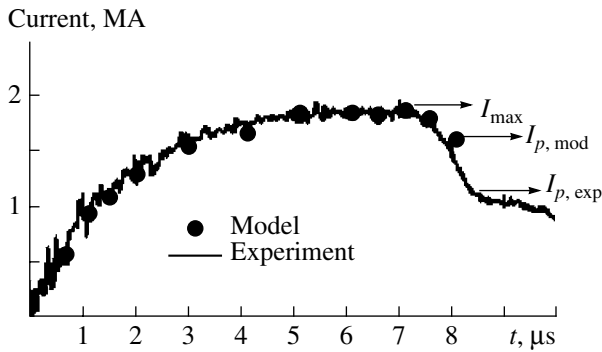


Fig. 3. Measured and calculated current waveforms.

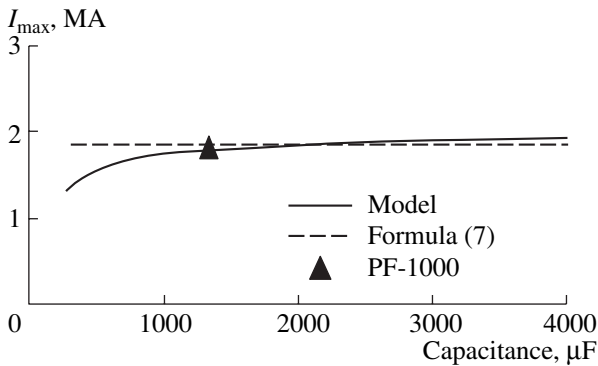


Fig. 4. Maximum current vs. capacitance of the energy storage bank.

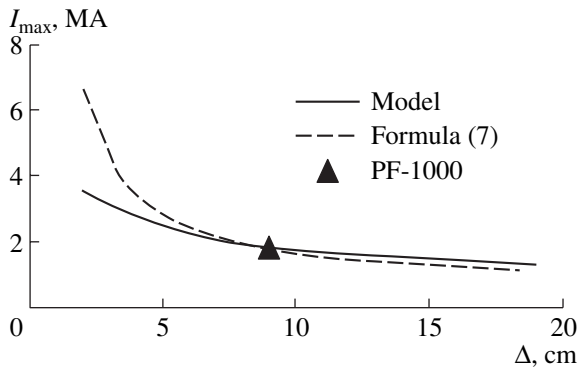


Fig. 5. Maximum current vs. electrode gap length Δ .

equal to the maximum current in the kilojoule energy range.

From Eqs. (4)–(6), we find the following estimate for the maximum current in the megajoule energy range:

$$I_{\max} = U_0 \frac{10^9}{\pi v_z \ln(R/r)}. \quad (7)$$

Let us substitute the facility parameters given the table into formula (7). Then, for the PF-1000 facility and the Frascati 1-MJ PF, we obtain $I_{\max} = 1.84$ and 2.19 MA, respectively. The fact that our rough estimate agrees unexpectedly well with the experimental results is rather surprising, because, in deriving formula (7), we only intended to reveal a qualitative dependence of the maximum current on the voltage and electrode geometry.

If we assume that $v_z = 10^7$ cm/s and $r \gg R - r = \Delta$, then formula (7) simplifies to

$$I_{\max} \approx 30U_0r/\Delta. \quad (8)$$

Thus, it follows from formulas (7) and (8) that the maximum discharge current in a megajoule PF depends only slightly on the capacitance of the energy storage bank and is mainly determined by the capacitor voltage and electrode diameters.

4. COMPARISON BETWEEN ANALYTIC RESULTS AND COMPUTER SIMULATIONS

To verify formulas (7) and (8) more thoroughly, we performed computer simulations of a discharge by using a version (from 1999) of the well-known two-fluid MHD code developed by Vikhrev et al. [8]. The code was tested against the measured time behavior of the current in PF-1000 [6] (Fig. 3). Without any refinement, the code provided good agreement between the calculated and measured values of the discharge current up to the middle of the CS radial compression phase; however, the pinch current I_p at the instant of maximum compression was overestimated by 20–30%.

In computer simulations, we verified the main consequences of formulas (7) and (8), such as the facts that the maximum current I_{\max}

(i) is independent of the capacitance of the energy storage bank (Fig. 4),

(ii) is inversely proportional to the electrode gap length (Fig. 5), and

(iii) depends linearly on the charging voltage of the capacitor bank (Fig. 6).

For this purpose, we varied the model parameters C , U_0 , and r , the electrode length l in each simulation version being chosen to provide the best matching between the capacitor bank and the discharge unit.

A discrepancy between the analytic results and computer simulations in Fig. 5 at $\Delta < 4$ cm is quite natural because, in this case, the chamber inductance is close to the inductance of the external circuit and, consequently, the above analytic approach is invalid. A discrepancy between the curves in Fig. 6 at voltages higher than 40 kV stems from the fact that, in the computer code, the CS axial velocity increased to higher than 10^7 cm/s, whereas in calculating by formula (7), this velocity was assumed to be constant and equal to I_p cm/s.

It is seen from Fig. 4 that, for the PF-1000 facility with the currently used electrode diameters, the discharge current is limited at a level of 2 MA, independently of the capacitance of the energy storage bank. At present, the PF-1000 capacitor bank consists of 260 5- μ F capacitors connected in parallel, each being capable of delivering more than 100 kA into the load but, actually, acting as an element of the facility, delivering no more than 7 kA. Thus, the electric current efficiency of the capacitor bank is less than 10%. Such a low efficiency, together with the dependence shown in Fig. 4, clearly illustrates the above considerations concerning current saturation in the megajoule energy range.

Thus, it can be seen from Figs. 4–6 that, on the whole, computer simulations agree well with formulas (7) and (8).

Let us now consider the energy scaling for the neutron yield. As was mentioned above, the current of a megajoule PF depends weakly on the stored energy and shows a tendency toward saturation. Taking into account scaling (2), this leads to the saturation of the neutron yield. In the kilojoule energy range, the neutron yield obeys scaling (1). Thus, there are two asymptotes for the energy scaling presented in Fig. 7. It can be seen that the results of computer simulations conform well to these analytic asymptotes. In simulations, the pinch current I_p was assumed to be equal to $I_p = (2/3)I_{\max}$ (see Fig. 3). Let us derive an analytic formula describing the saturation of the neutron yield in the megajoule energy range (Fig. 7). First, we determine the energy dependence of the maximum current in the transition part of the curve (at ~ 0.1 MJ) and substitute it into scaling (2). We assume that, in this energy range, the chamber inductance is comparable with the inductance of the feeding cables, so the maximum current is determined by the sum of these inductances,

$$I_{\max} \approx U_0 \sqrt{\frac{C}{L_f + L_c}}. \quad (9)$$

Assuming that nearly one-half of the stored energy is converted into the energy of the magnetic field in the interelectrode space (i.e., $L_f \approx E/I_{\max}^2$) and that $I_p = (2/3)I_{\max}$, we obtain the following energy scaling for the neutron yield:

$$Y_n \approx \frac{10^{-13}}{L_c^2} \left(\frac{E}{1 + E/(L_c I_{\max}^2)} \right)^2 \sim \left(\frac{E}{1 + \alpha E} \right)^2, \quad (10)$$

$$\alpha = \frac{1}{L_c I_{\max}^2} \approx \text{const},$$

where I_{\max} is determined by formulas (7) and (3) for the mega- and kilojoule energy ranges, respectively; E is the energy stored in the capacitor bank; and L_c is the inductance of the capacitor bank and feeding cables. Formula (10) represents the energy scaling for the neutron yield in both the kilo- and megajoule energy

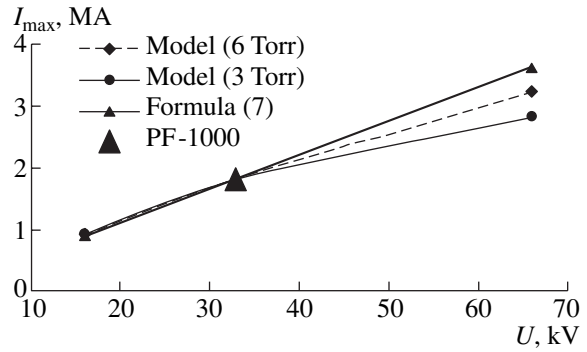


Fig. 6. Maximum current vs. charging voltage U .

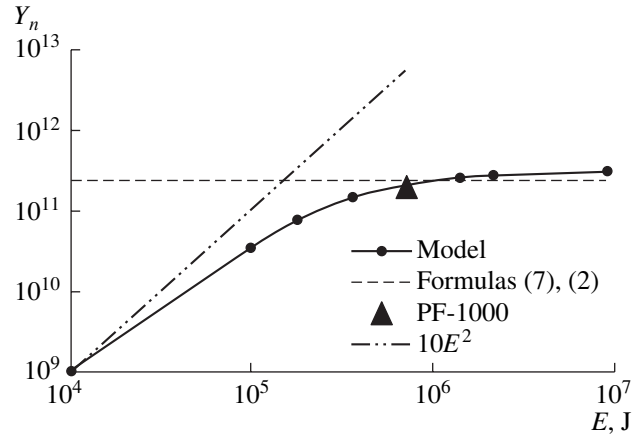


Fig. 7. Neutron yield Y_n vs. stored energy E .

ranges. According to this formula, the neutron yield is governed by the parameters of the capacitor bank (U , C , and L_c) and the chamber (R , r). Indeed, in the kilojoule energy range, we have $L_c \sim 10^{-7}$ nH and the denominator in the parentheses is on the order of unity, so the neutron yield is $Y_n \sim 10E^2$. In the megajoule energy range, the unity in the denominator can be ignored, so we have $Y_n \approx \text{const}$; i.e., the neutron yield saturates. Thus, formula (10) describes the asymptotic behavior of the neutron yield with increasing stored energy. Note that this neutron scaling represents a set of curves corresponding to different values of the parameter $\alpha = \text{const}$, which is determined by the main parameters of a facility (Fig. 8). According to formula (7), the higher the maximum discharge current, the higher the corresponding curve.

Hence, instead of inefficiently increasing the storage energy, a further increase in the neutron yield can be achieved by increasing the charging voltage of the capacitor bank and/or to decreasing the electrodes gap length in accordance with formulas (7) and (8).

To some extent, this approach has already been verified experimentally. For example, three high-power

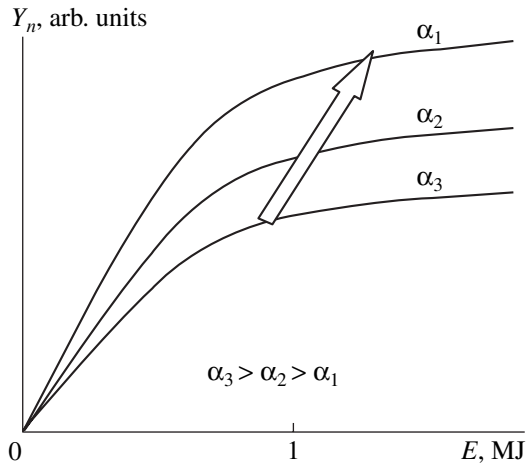


Fig. 8. Neutron yield Y_n vs. stored energy E for different α values.

Mather-type PFs with an increased charging voltage, specifically, the Poseidon (80 kV, 500 kJ), Speed 1 (200 kV, 30 kJ), and Speed 2 (300 kV, 200 kJ) facilities, were constructed in Germany. However, the maximum neutron yield in these facilities did not exceed 10^{11} . According to [9, 10], the main obstacle was the PF insulator, from which too much impurities were evaporated into the discharge. To prevent this, glass insulators at the Poseidon facility were replaced with ceramic ones. To increase the stored energy and the neutron yield in the Speed 2 facility, the insulator diameter and, accordingly, the electrode diameters were increased for reasons of maintaining the energy load per unit area of the insulator at a constant level. Not casting any doubt on this approach, we can say that, according to formula (8), an increase in the insulator diameter should also lead to an increase in the discharge current. Thus, both the experimental and theoretical results show that the PF current can be increased by increasing the electrode diameter. This approach automatically leads one to a Filippov-type PF.

5. FILIPPOV-TYPE PF

The considerations used in deriving formulas (7) and (8) also apply to a Filippov-type PF. However, it should be kept in mind that, for this type of PF, the chamber inductance in the megajoule energy range is relatively low and the major role is played by the pinch inductance:

$$L_p = 2h \ln(R/r_p), \quad (11)$$

where h is the pinch height and r_p , R , and r are the radii of the pinch, cathode, and anode, respectively (Fig. 1).

Let us assume for estimates that $R \sim r \sim 100$ cm and $r_p \sim 1$ cm; then, we have $\ln(R/r_p) \approx 4$ and $L_p \approx 8h$. For a pinch of height $h \approx 5$ cm, its inductance is $L_p \approx 40$ nH,

whereas the inductances of the capacitor bank and the chamber are $L_c \sim L_f \sim 10\text{--}20$ nH (see table).

The current rise time t is comparable to the time of CS radial compression:

$$t = \frac{\pi}{2} \sqrt{L_p C} \approx r/v_r \approx h/v_z, \quad (12)$$

where v_r is the CS radial velocity and v_z is the CS axial velocity in the stage of radial compression.

Simple manipulations similar to those performed in deriving formulas (4)–(8) lead to the following expression for the maximum discharge current:

$$I_{\max} \approx 10^8 U/v_z \approx 10^8 U r/(h v_r) = 10^8 U t/h. \quad (13)$$

Let us apply formula (13) to the PF-3 facility, which is currently the largest Filippov-type device (see table). Assuming that the pinch height is $h \approx 5$ cm, we find that the maximum current I_{\max} in the PF-3 facility is equal to

$$I_{\max} [\text{A}] \approx 300U [\text{V}]. \quad (14)$$

For charging voltages of $U = 12\text{--}15$ kV, we have $I_{\max} = 3.6\text{--}4.5$ MA, which is comparable to the experiment data (see table).

It is of interest to derive relationships similar to formula (14) for the above high-power Mather-type facilities. Using formula (7) and the data from the table, we find that, for the PF-1000 facility,

$$I_{\max} [\text{A}] \approx 60U [\text{V}]. \quad (15)$$

and, for the Frascati 1-MJ PF,

$$I_{\max} [\text{A}] \approx 80U [\text{V}]. \quad (16)$$

A comparison of formulas (14)–(16) shows that Filippov-type PFs are more preferable from the electrotechnical standpoint.

Unfortunately, the computer code employed is incapable of simulating the discharge dynamics in Filippov-type PFs, so we failed to obtain the dependences analogous to those in Figs. 4–6. Nevertheless, it can be seen from formula (13) that, for a Filippov-type PF, the discharge current in the megajoule energy range is also independent of the capacitance of the energy storage bank. Formula (13) determines the position of the horizontal asymptote in the neutron scaling similar to that shown in Fig. 7. A comparison of formulas (14)–(16) shows that, for Filippov-type PFs, the family of curves (similar to those in Fig. 8) should lie above those for Mather-type PFs.

In practice, however, the neutron yield in Filippov-type facilities is no higher and is sometimes even lower than that in other types of PF. The reason for this is yet unclear; it is known, however, that Filippov-type facilities are less stable in operation and that troubles with such facilities grow with increasing the insulator area. Let us point to another feature. In a Mather-type PF, the energy stored in the capacitor bank is first converted into the magnetic energy of the chamber (the chamber inductance) and the rest of energy is converted into the

magnetic energy of the pinch. For example, computer simulations of the PF-1000 facility show that, by the instant of singularity in the current time derivative, about one-half of the energy remains in the capacitor bank, one-fourth of energy is converted into the magnetic energy of the chamber, and one-fourth is converted into the magnetic energy of the pinch. In a Filippov-type PF, the intermediate stage is absent and, accordingly, the discharge current is higher. However, it well may be that, in a Mather-type PF, the chamber inductance plays the role of a stabilizing energy reservoir that supplies the discharge at the instant of singularity.

Note that the conclusion about the saturation of the neutron yield in the megajoule energy range was obtained within a rather rough electrotechnical approach, without considering physical mechanisms for neutron generation. Moreover, the fact that the discharge inductance depends on time was ignored. Nevertheless, this approach agrees well with both computer simulations and experimental results. Probably, the above assumption that the pinch current is rigidly related the maximum current, $I_p = (2/3)I_{\max}$, is not quite justified. In real discharges, the relation between these currents is, of course, different for different facilities (see table) and varies from shot to shot. We also left aside the question of shunting the main current. However, a detailed consideration of these problems goes beyond the scope of the electrotechnical approach developed here.

6. CONCLUSIONS

At first glance, the experimental data acquired over the past few decades by merely increasing the PF energy without optimizing the discharge chamber lead to pessimistic predictions concerning the use of PFs as high-power sources of thermonuclear neutrons. Such a disappointment, however, seems to be not quite justified. As was shown above, the point is that present-day Mather-type facilities are simply incapable of providing a larger neutron yield. It is clear now that further progress in increasing the neutron yield can be achieved by improving the electrode geometry and simultaneously elevating the charging voltage of the capacitor bank rather than by merely increasing the stored energy. In this context, the prospects of using Filippov-type PFs in the megajoule energy range look more optimistic, although this type of PF has been little studied

yet because there has been only one such facility operating at relatively low voltages and only with heavy gases.

ACKNOWLEDGMENTS

We are grateful to V.V. Vikhrev for kindly providing us with the computer code and for useful discussions. This study was supported in part by the program of the Division of Physical Sciences of the Russian Academy of Sciences "Problems of Plasma Stability and Reaching the Ultimate Plasma Parameters in Magnetic Confinement Systems," the Russian Foundation for Basic Research (project no. 06-02-17398), and the RF Ministry of Science and Education under the Program for State Support of Leading Scientific Schools (grant no. NSh-5489.2006.2).

REFERENCES

1. J. Pouzo, in *Proceedings of the 2nd Symposium on Current Trends in International Fusion Research, Washington, DC, 1997*, Ed. by E. Panarella (NRC Research Press, Ottawa, 1999), p. 41.
2. H. Schmidt, Report No. IPF-87-5 (Institut für Plasmaforschung, Stuttgart, 1987).
3. V. A. Burtsev, V. A. Gribkov, and T. I. Filippova, *Itogi Nauki Tekh., Ser. Fiz. Plazmy* **2**, 226 (1981).
4. C. Goulland, H. Kroegler, Ch. Maisonnier, et al., Preprint No. 78.12/cc (CNEN Frascati Center, Roma, 1978).
5. V. Ya. Nikulin, S. N. Polukhin, and A. A. Tikhomirov, *Fiz. Plazmy* **31**, 642 (2005) [*Plasma Phys. Rep.* **31**, 591 (2005)].
6. M. Sholz, in *Proceedings of the Workshop and Expert Meeting of the International Centre for Dense Magnetized Plasma, Warsaw, 2004*, p. 210.
7. M. A. Karakin, E. Yu. Khautiev, V. I. Krauz, et al., in *Proceedings of the 15th International Conference on High-Power Particle Beams, St. Petersburg, 2004*, p. 7014.
8. V. V. Vikhrev, V. V. Ivanov, and G. A. Rosanova, *Nucl. Fusion* **33**, 311 (1993).
9. W. Kies, *Plasma Phys. Controlled Fusion* **28**, 1645 (1986).
10. H. Schmidt, H. Herold, L. Bertalot, et al., *Atomkernenerg. Kernt.* **44**, 191 (1984).

Translated by N.N. Ustinovskii